Nigerian Research Journal of Engineering and Environmental Sciences 2(1) 2017 pp. 18-31

Nigerian Research Journal of Engineering and Environmental Sciences
Journal homepage: www.rjees.com

Original Research Article

POLARISATION MODELLING OF AN ANODE SUPPORTED SOLID OXIDE FUEL CELL

[1,2]*Ighodaro, O. and [2]Keith, S.

[1]Department of Mechanical Engineering, Faculty of Engineering, University of Benin, Benin City, Nigeria.
[2]School of Chemical Engineering and Advanced Materials, Newcastle University, UK.
*osaighodaro@gmail.com

ARTICLE INFORMATION

Article history:
Received 14 February 2017
Revised 22 March 2017
Accepted 22 March 2017
Available online 01 June 2017

Keywords:
Polarisation
Anode support
Intermediate temperature
Activation
Ohmic

ABSTRACT

A polarisation model was developed and validated for an intermediate temperature anode-supported solid oxide fuel cell (SOFC). The model was used to analyse the effects of activation, concentration and ohmic polarisation on the overall polarisation in the cell. The electrochemical active layer was modelled as a distinct electrode layer. The modified Butler-Volmer equation which incorporates the Knudsen diffusion term was used in calculating the activation and concentration polarisation terms while ohms law was used in calculating the cell resistance. The simulation results showed that the activation polarisation and the ohmic polarisation were the most significant contributors to the overall voltage loss in the cell and the magnitude of the concentration polarisation for each distinct layer is dependent on the thickness of the electrode layer.

1. INTRODUCTION

Solid oxide fuel cells (SOFCs) are attracting significant research attention in recent times because of their huge potentials for power generation in stationary, portable and transport applications and their high energy conversion efficiency when compared to other fuel cells (Singhal and Kendall, 2003; Larminie et al., 2003; Chinda et al., 2010). In addition, internal reforming of hydrocarbons can be carried out in the anode and they have significantly lower emissions of sulphur oxides, nitrogen oxides and carbon dioxide compared to conventional power generation devices (Yakabe et al., 2001; Staniforth and Ormerod, 2002; Andersson et al., 2012). Conventional power generation is based on either the gas power cycles or the vapour power cycles; with their maximum thermal efficiencies limited by the Carnot cycle. However, due to the ability of SOFCs to be integrated with gas turbine units and their

corresponding increased efficiency, this integrated solid oxide fuel cells-gas turbine (SOFC-GT) units are been identified as a more advanced technology for future power generation (Ormerod, 2003). With the SOFC stack contributing a significantly larger amount of the total electric power output, there is an important need to study the performance of the cell which is affected by the various polarisation losses.

There are three major loss mechanisms in SOFCs which results in the loss of useful voltage of at a given operating current density, these are the activation polarisation, concentration polarisation and ohmic polarisaation. At specific operating conditions, these polarisation losses are largely dependent on cell materials, electrode microstructure and cell geometry. The activation polarisation originates from the irreversibility associated with the sluggishness of the electrochemical reaction to proceed while the concentration polarisation originates from the irreversibility associated with mass diffusion process of the reactants. Due to the fast kinetic reactions in SOFCs as a result of its high temperature operations, the modified Butler-Volmer equation is used in solving for the activation and concentration polarisation (Aguiar et al., 2004). The ohmic polarisation is the voltage loss due to the ohmic resistance of the electrolyte and electrodes. In practice, the active reaction layer (triple phase boundary TPB) is often neglected or lumped into the exchange current density term, however (Hussain et al., 2006) and (Ni et al., 2007) found out that it also significantly affects the polarisation values. An efficient operation of the SOFC requires that all of these losses be as small as possible. The processes influencing the performance of SOFCs are complex and multidiscipline. Carrying out experiments to investigate them can be quite expensive and time consuming. With the use of some key results and parameters obtained from experimental works, a detailed accurate model can be constructed, and this model can then be used to analyse the performance of the cell.

Consequently, this study aims to develop a detailed two dimensional polarisation model of an anode supported SOFC which will be used to analyse the effect and contributions of the activation, concentration and ohmic polarisation to the overall polarisation loss in the cell.

2. DESCRIPTION AND OPERATION OF FUEL CELL

A schematic of the cell as shown in Figure 1 composed of a thin electrolyte layer sandwiched between the thick anode electrode layer (made up of the anode diffusion layer (ADL) and the anode reaction layer (ARL)) and thin cathode electrode layer (made up of the cathode diffusion layer (CDL) and the cathode reaction layer (CRL). The model consists of seven sub domains namely: anode channel (ACH), ADL, ARL, electrolyte, CRL, CDL and cathode channel (CCH). The SOFC cell is supported on the thick anode diffusion layer. The oxygen (O_2) gas diffuses through the cathode to the CRL where the electrochemical reduction reaction occurs, and the reduced oxygen ions then migrates through the electrolyte to the ARL.

$$\frac{1}{2}O_2 + 2e^- \rightarrow O^{2-} \quad (1)$$

The hydrogen (H_2) gas diffuses through the porous anode support layer to the ARL where the following electrochemical reaction occurs:

$$H_2 \rightarrow 2H^+ + 2e^- \quad (2)$$

$$2H^+ + O^{2-} \rightarrow H_2O \quad (3)$$

The reaction product H_2O then diffuses back into the fuel channel. The entire reaction process occurs in three main steps. The first is the diffusion of the reactants through the channels and diffusion layers to the reaction layers. The second step is the electrochemical reaction which takes place in the reaction layers and the final step is the diffusion of the products into the channel through the diffusion layer.

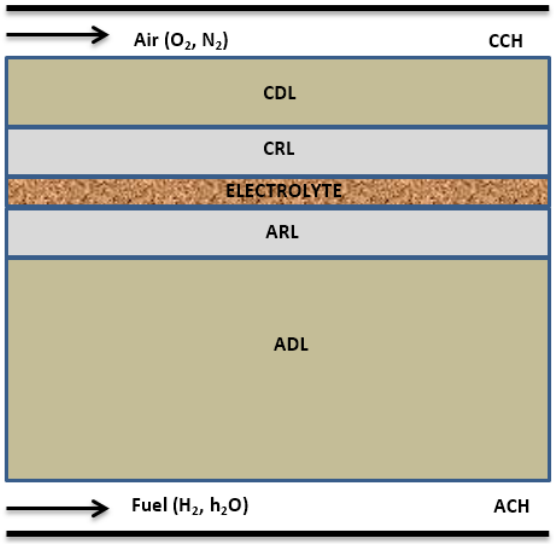

Figure 1: Schematic of anode supported SOFC

3. MODEL DEVELOPMENT AND IMPLEMENTATION

The finite element commercial software COMSOL Multiphysics (version 4.3a) is used to solve and analyse the non-linear system of governing equations and boundary conditions described above. The software is designed to solve sets of coupled algebraic and differential equations. The computational geometry consists of 333,742 degrees of freedom and 120,196 elements, and the distance between each element is known as a step. At each step, the equations accounting for each phenomenon are fully coupled and computed as shown in the schematic in Figure 2. The convergence of the numerical solutions was judged by the relative tolerance criteria of 1×10^{-4}. The cell geometry consisted of a 1000µm thick nickel- yittria stabilized zirconia (Ni-YSZ) anode diffusion and an additional 20 µm anode reaction layer. The electrolyte was a 10µm thick layer of YSZ while the cathode consisted of a 20 µm thick layer of strontium doped lanthanum manganite (LSM)-YSZ with a buffer layer of 50 µm LSM.

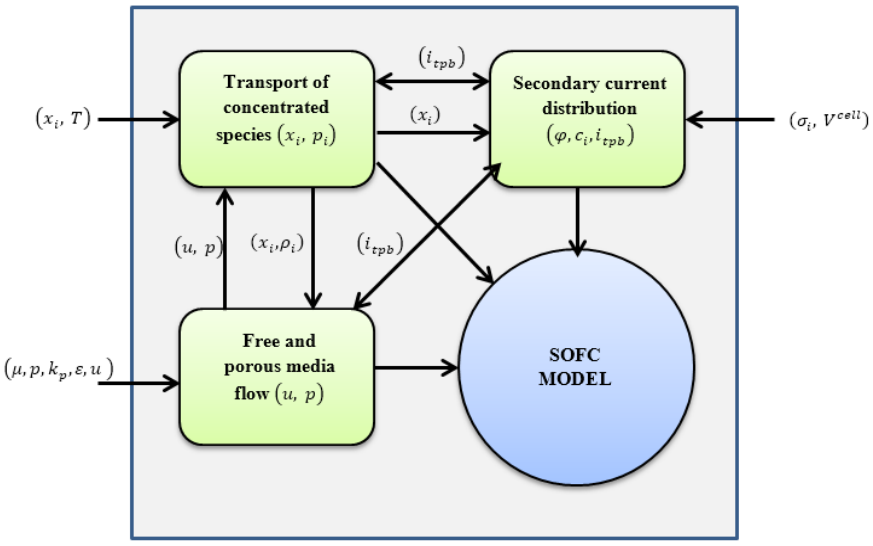

Figure 2: Schematic of computational process

The major assumptions used in developing the model include:

- The air and fuel are supplied in the co-flow arrangement
- The SOFC operates under steady state conditions
- Wall boundaries are at constant temperature
- Temperature and pressure are uniform in the electrode layers
- Reactant gas mixtures are ideal gases with negligible viscous and gravity effects
- Electrochemical reactions occur only in the reaction layers
- The reaction layers consist of a mixture of electron conducting particles, electrolyte conducting particles and void spaces occupied by gaseous species
- The conducting particles were equal sizes
- Knudsen diffusion term was neglected
- Electrolyte is a dense layer with no porosity.
- Gas flow profiles are laminar

On the basis of these assumptions, the model was formulated as shown in the following sections.

3.1. Momentum Transport

The reactants flows to the reaction layers where the electrochemical reactions takes place, this flow usually results in pressure drops along the transport direction. The traditional modelling approach for this phenomena is to use the Navier-stokes equations for the channels and the Darcy equations for the porous region (substrate and functional layers). Using this approach entails defining complex interfacial conditions for the velocity and pressure flow at the boundary between the channel and electrodes. The Darcy-Brinkman equation (Andersson *et al*., 2012) is introduced to overcome this problem as it can solve for gas flow in air and fuel channel.

$$\left(\frac{\mu}{pe} + \rho.\boldsymbol{u}.\nabla\right).\boldsymbol{u} = \nabla.[-p+\mu\,\Psi - \frac{2}{3}\mu(\nabla.u)] = F \quad (4)$$

Where F is the generic body force (gravity or volume forces), pe is the permeability of the porous medium, ε_p is the porosity, u is the velocity vector, Ψ is the viscous stress tensor, μ is the viscosity and p is the pressure. The dynamic viscosity for the participating gases was evaluated as:

$$\mu_i = \sum_{k=0}^{6} b_k \cdot \left(\frac{T}{1000}\right)^k \quad (5)$$

$$\mu_g = \sum_i x_i.\mu_i \quad (6)$$

b_k is the species dependent parameter, k is the number of species dependent parameter in the viscosity equation and x is the species mass fraction. The gas inlet velocities are defined as laminar flow profiles.

3.2. Mass Transport

The mass transport in the fuel cell was modelled using the Maxwell-Stefan equations (Hussain et al., 2006) for diffusion and convection, which solves for molecular diffusion i.e. collision between gas molecules as the Knudsen diffusion term which accounts for the collision between the gas molecules and the solid wall is neglected. The Maxwell-Stefan equation solved for the fuel and air channels and electrodes is given by:

$$\nabla \cdot \underbrace{\left\{-\rho w_i \sum_{j=1}^{N} D_{ij}\left[\frac{M_n}{M_j}\left(\nabla w_j + w_j \frac{\nabla M_n}{M_n}\right) + \left(x_j - w_j\right)\frac{\nabla p}{p}\right]\right\}}_{\text{Diffusion}} + \underbrace{(\rho \mathbf{u} \cdot \nabla w_i)}_{\text{Convection}} = 0 \quad (7)$$

w_i, the mass fraction of the specie i and D_{ij} is the Maxwell-Stefan diffusion coefficient. The effective diffusion coefficient$\left(D_i^{eff}\right)$ in the porous region of the cell was defined as shown in Equation 8 (Andersson et al., 2012):

$$D_i^{eff} = \varepsilon_p {D_{ij}}^{1.5} \quad (8)$$

The molecular diffusion coefficient D_{ij} is calculated using the Fuller equation for binary diffusion coefficient given in Equation 9 (Hussain et al., 2006):

$$D_{ij} = \frac{0.00143.T^{1.75}}{p.M_{ij}^{1/2}.\left({v_i}^{1/3} + {v_j}^{1/3}\right)} \quad (9)$$

$$M_{ij} = \frac{2}{\frac{1}{M_i}+\frac{1}{M_j}} \quad (10)$$

Where M_i the molar is mass and v_i is the Fuller diffusion volume.

3.3. Ion and Electron Transport

3.3.1. Diffusion layers

The diffusion layer is a purely electronic conductive layer and the processes that need to be modelled in this is the electron migration. The mathematical model was formulated by applying the conservation of electronic charge. The equation is given by:

$$\nabla . i_s = 0 \tag{11}$$

$$i_s = \sigma_{dl}^{eff} \nabla \varphi_e \tag{12}$$

φ_e is the potential and σ_{dl}^{eff} is the effective electronic conductivity of the electrode diffusion layers was calculated from Equation 13:

$$\sigma_{dl}^{eff} = \left(\frac{1-\varepsilon_p}{\tau}\right)\sigma \tag{13}$$

where σ is the electronic conductivity of the diffusion layer material:

$$\sigma_{s,a} = \frac{9.5 \,.\, 10^7}{T} \,.\, exp\left(\frac{-1150}{T}\right) \tag{14}$$

$$\sigma_{s,c} = \frac{4.2 \,.\, 10^7}{T} \,.\, exp\left(\frac{-1200}{T}\right) \tag{15}$$

$\sigma_{s,a}$ is the anode electronic conductivity, $\sigma_{s,c}$ is the cathode electronic conductivity and T is the operating temperature.

3.3.2. Reaction layers

The reaction layers are very thin layers having mixed electronic and ionic conductive properties in which fuel and air are electrochemically converted into electricity, heat and water. The process which needs to be modelled is the electron and ion migration in the respective conducting particles. The equations governing this migration are defined as follows:

Anode reaction layer

Electronic charge: $\nabla . i_s = R_a$ (16)

Ionic charge: $\nabla . i_i = -R_a$ (17)

Cathode reaction layer

Electronic charge: $\nabla . i_s = -R_c$ (18)

Ionic charge: $\nabla . i_i = R_c$ (19)

Where $i_i \; and \; i_s$ are the ionic and electronic current densities respectively given by:

$$i_i = k_{rl}^{eff} \nabla \varphi_i \tag{20}$$

$$i_s = \sigma_{rl}^{eff} \nabla \varphi_s \tag{21}$$

$$k_{rl}^{eff} = \emptyset \left(\frac{1-\varepsilon_p}{\tau}\right) k_{el} \tag{22}$$

$$\sigma_{rl}^{eff} = \emptyset \left(\frac{1-\varepsilon_p}{\tau}\right) \sigma \tag{23}$$

Where $\emptyset$ is the volume fraction of the electron conducting particles, k_{el} and σ are the conductivities of pure ion and electron conducting particles respectively, $k_{el}$was calculated as follows:

$$k_{el} = 33.4 \,.\, 10^3 \,.\, exp\left(\frac{-10300}{T}\right) \tag{24}$$

R_a and R_c are the volumetric current densities defined by the general Butler-Volmer equation (Hussain et al., 2006) as:

$$R_a = A_V i_{0,ref}^{H_2} \left(\frac{c_{H_2}}{c_{H_{2,ref}}}\right)^{\gamma H_2} * \left[exp\left(\frac{\alpha n F \eta_a}{RT}\right) - exp\left(\frac{-(1-\alpha) n F \eta_a}{RT}\right)\right] \tag{25}$$

$$R_c = A_V i_{0,ref}^{O_2} \left(\frac{c_{O_2}}{c_{O_{2,ref}}}\right)^{\gamma O_2} * \left[exp\left(\frac{\alpha n F \eta_c}{RT}\right) - exp\left(\frac{-(1-\alpha) n F \eta_c}{RT}\right)\right] \tag{26}$$

Where A_V is the actual reactive surface area per unit volume, $i_{0,ref}^{H_2}$ and $i_{0,ref}^{O_2}$ are the reference exchange current densities for hydrogen oxidation and oxygen reduction at the reference concentrations, α is the charge transfer coefficient, n is the number of participating electrons in the electrochemical reaction, η_a and η_c are the anode and cathode activation polarisation defined as:

$$\eta_a = \varphi_s - \varphi_i - E_{eq,a} \tag{27}$$

$$\eta_c = \varphi_s - \varphi_i - E_{eq,c} \tag{28}$$

Costamagna et al. (1998) developed the expression used in modelling the reactive surface area per unit volume A_V, given as:

$$A_V = \pi sin^2\theta {r_{el}}^2 n_t n_{el} n_{io} \frac{Z_{el} Z_{io}}{Z} \, p_{el} p_{io} \tag{29}$$

Where θ is the contact angle between electron and ion conducting particles in the functional layer, r_{el} is the radius of the electron conducting particle, n_t is the total number of particles per unit volume, n_{el} and n_{io} are the number fraction of electron and ion conducting particles in the functional layer respectively, Z_{el} and Z_{io} are the number of electron and ion conducting particle, Z is the total average number of contacts of each particle, p_{el} and p_{io} are the probalilities of electron and ion conducting particles in the functional layer. The parameters required to obtain A_V were calculated thus:

$$n_t = \frac{1-\varepsilon_p}{(4/3)\pi r_{el}^3\left[n_{el}+(1-n_{el})\left(r_{io}/r_{el}\right)^3\right]} \quad (30)$$

$$n_{el} = \frac{\emptyset}{\left[\emptyset+\left(\frac{(1-\emptyset)}{\left(r_{io}/rel\right)^3}\right)\right]} \quad (31)$$

$$n_{io} = 1 - n_{el} \quad (32)$$

$$Z_{el} = 3 + \frac{Z-3}{\left[n_{el}+(1-n_{el})\left(r_{io}/r_{el}\right)^2\right]} \quad (33)$$

$$Z_{io} = 3 + \frac{Z-3\left(r_{io}/r_{el}\right)^2}{\left[n_{el}+(1-n_{el})\left(r_{io}/r_{el}\right)^2\right]}c \quad (34)$$

$$p_{el} = \left[1-\left(2-\frac{Z_{el-el}}{2}\right)^{2.5}\right]^{0.4} \quad (35)$$

$$p_{io} = \left[1-\left(2-\frac{Z_{io-io}}{2}\right)^{2.5}\right]^{0.4} \quad (36)$$

where $Z_{el-el} = \frac{n_{el}Z_{el}^2}{Z}$ (37)

$$Z_{io-io} = \frac{n_{io}Z_{io}^2}{Z} \quad (38)$$

3.3.3. Electrolyte layer

The function of the electrolyte is to conduct the oxide ions produced in the cathode reaction layer to the anode reaction layer so as to complete the electrical circuit. The layer is fully dense. The equation governing the migration of the oxide ion is given by:

$$\nabla . i_i = 0 \quad (39)$$

Where i_i is the ionic current density given by Equation (40).

$$i_i = k\nabla\varphi_i \quad (40)$$

3.5. Boundary Conditions

In solving the model, a number of parameters have to be defined at the interfaces (boundary conditions), these parameters are the mass fraction (continuity equation) and characteristics of flow field i.e. velocity or pressure (momentum equation). The molar fraction of the

participating gases at the inlet also had to be specified. The Darcy-Brinkman equation makes it possible to define the interface between the flow channels and the porous electrodes as continuous. The pressure/velocity of the gas was specified at the inlet and outlet. The velocity of the gases is zero at the channel wall. The mathematical expression for the boundary condition at different locations in the cell can be expressed as:

$$(\rho u.\nabla w_i + \nabla m_i).n|_{gas\ channel} = -(\varepsilon_p \rho u.\nabla w_i + \nabla m_i).n|_{diffusion\ layer} \quad (41)$$

$$i_s.n = 0|_{channel-diffusion\ layer} \quad (42)$$

$$i_i.n = 0|_{channel-diffusion\ layer} \quad (43)$$

$$(\varepsilon_p \rho u.\nabla w_i + \nabla m_i).n|_{diffusion} = -(\varepsilon_p \rho u.\nabla w_i + \nabla m_i).n|_{reaction} \quad (44)$$

$$(i_s.n)_{diffusion\ electrode} = (i_i.n + i_s.n)_{reaction\ electrode} \quad (45)$$

$$(i_i.n + i_s.n)_{reaction\ electrode} = (i_i.n)_{electrolyte} \quad (46)$$

$$i_i.n = 0|_{electrolyte-reaction\ layer} \quad (47)$$

4. MODEL VALIDATION

The range of validity and accuracy of the hydrogen fed SOFC model was determined by comparing experimental data with the numerically developed cell performance result. To carry out the validation, experimental data from Jung et al. (2006) was utilised. Figure 3 compares this model predicted results with that obtained from the experimental data of Jung et al. (2006) at 1073K. The parameters used for the model simulation are listed in Table 1. Most of the parameters used in validating the model were obtained from Jung et al. (2006) while other parameters not provided by the experimental report were obtained from literature.

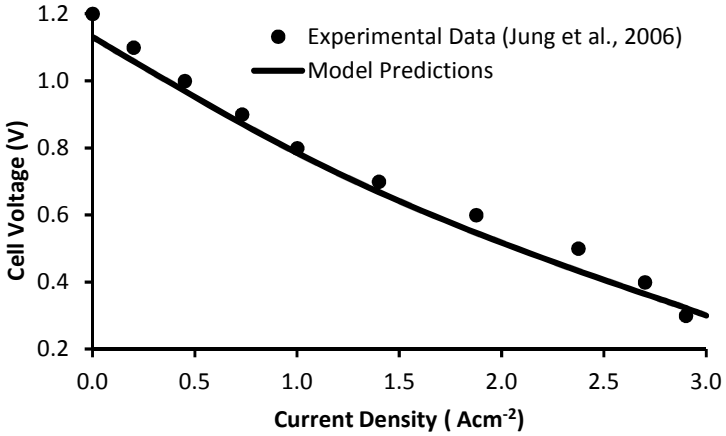

Figure 3: Comparison between model prediction and experiment

As seen in Figure 3, there was good agreement between the experimental results and the model prediction. The geometric and permeability values used in the simulation were those

reported in Jung et al 2006. Other parameters used were either estimated or calculated. The tortuosity value was varied to obtain the best agreement between experimental result and model prediction. Literature suggests typical values in the range of 2-10 (Hussain et al., 2006, Chinda et al., 2010).

Table 1: Parameters and properties used in validating the model

Parameters	Value
Flow channels	
Layer thickness $l_{ch}(\mu m)$	1000
Cell Length, $t_{ch}(\mu m)$	50000
Anode diffusion layer (ADL)	
Layer thickness, $l_{adl}(\mu m)$	1000
Pore diameter, $d_{pore,adl}(\mu m)$	1.4
Porosity, ε_{adl}	0.42
Volume fraction, φ_{adl}	0.4
Permeability, $K_{adl}(*10^{-12}m^2)$	0.034
Effective conductivity,$\sigma_{adl}(S\ cm^{-1})$	1011
Anode reaction layer (ARL)	
Layer thickness, $l_{arl}(\mu m)$	20
Pore diameter, $d_{pore,arl}(\mu m)$	0.33
Porosity, ε_{arl}	0.097
Volume fraction, φ_{arl}	0.4
Permeability, $K_{arl}(*10^{-12}m^2)$	0.034
Effective conductivity,$\sigma_{arl}(S\ cm^{-1})$	1011
Cathode diffusion layer (CDL)	
Layer thickness $l_{cdl}(\mu m)$	13
Pore diameter, $d_{pore,cdl}(\mu m)$	1.4
Porosity, ε_{crl}	0.36
Volume fraction, φ_{cdl}	1
Permeability, $K_{arl}(*10^{-12}m^2)$	0.037
Effective conductivity,$\sigma_{arl}(S\ cm^{-1})$	152
Cathode reaction layer (CRL)	
Layer thickness $l_{crl}(\mu m)$	25
Mean particle diameter, $d_{pore,crl}(\mu m)$	2
Porosity, ε_{crl}	0.4
Volume fraction, φ_{crl}	0.587
Permeability, $K_{arl}(*10^{-12}m^2)$	0.054
Effective conductivity,$\sigma_{arl}(S\ cm^{-1})$	93
Electrolyte (E)	
Layer thickness $l_e(\mu m)$	8
Effective conductivity,$\sigma_{arl}(S\ cm^{-1})$	0.047
Operating conditions	
Operating temperature, $T(K)$	1073K
Total pressure, $p(atm)$	1.0
Fuel inlet composition, x_{H_2} ; x_{H_2O}	0.97; 0.03
Air inlet composition, x_{O_2} ; x_{N_2}	0.21; 0.79

5. RESULTS AND DISCUSSION

The performance and contribution of each polarisation at 800°C is shown in Figure 4, the maximum power density (MPD) was obtained as 1.04 Wcm^{-2} at a current density of 2.08 Acm^{-2} and cell voltage of 0.5V. The activation polarisation in the cathode is seen to be dominant amongst other potential losses. SOFCs are usually designed to operate at cell voltage between 0.6 and 0.7V. Under such conditions, the best operating points would be current densities between 1.61 and 1.2 A cm^{-2} and power densities between 0.98 and 0.87 W cm^{-2}. At cell voltage of 1V (0.3 A cm^{-2}), the contribution of the cathode polarisation to the overall voltage loss was 72% (all activation), while that of the anode amounts to 28% (all activation), when the cell voltage reduced to 0.7V (1.2 A cm^{-2}), the cathode potential losses reduces to 64% (all activation), the anode amounted to 21% (concentration is 16% and activation 5%) while the electrolyte increases to 15%. The significant contribution of the cathode polarisation is due to the sluggishness of the oxygen reduction reaction and the presence of ionic conducting particles in the reaction layer of the cathode.

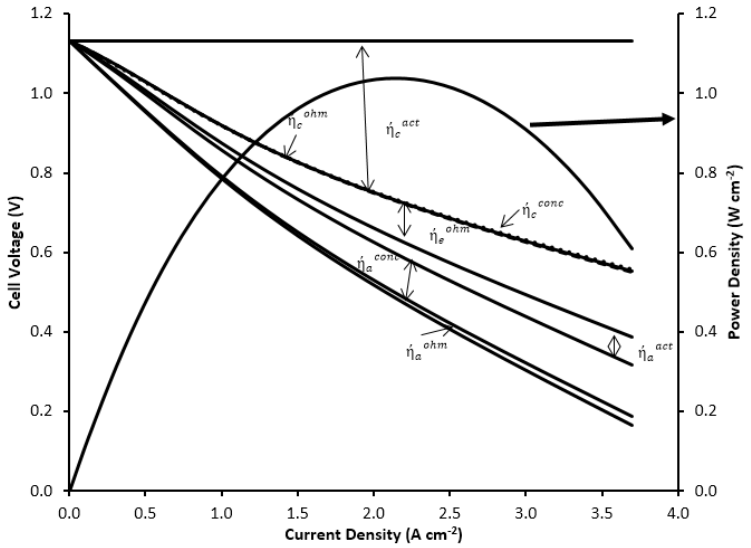

Figure 4: I-V and I-P performance with contributions of each polarisation

Figures 5 and show the polarisation from the anode and cathode side with the anode concentration polarisation been the most significant on the anode side due to the large anode diffusion layer while on the cathode side is the activation polarisation due to its sluggishness. The ohmic polarisation on both sides is not that significant due to the thin reaction layers.

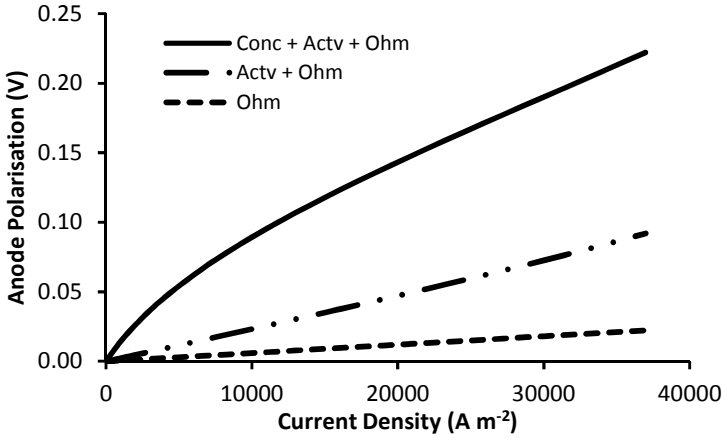

Figure 5: Anode side polarisation as a function of current density

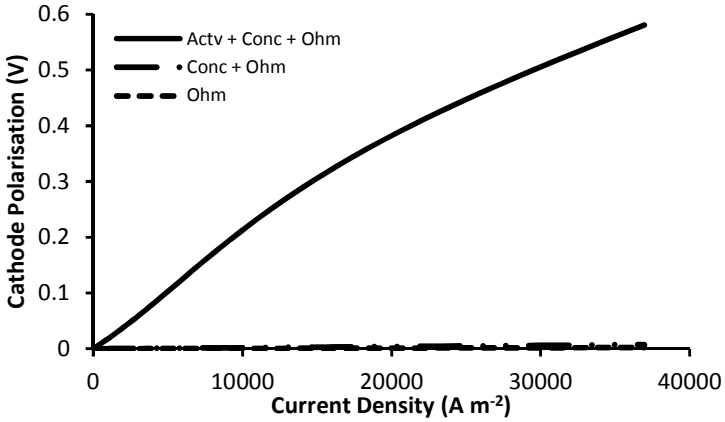

Figure 6: Cathode polarisation as a function of current density

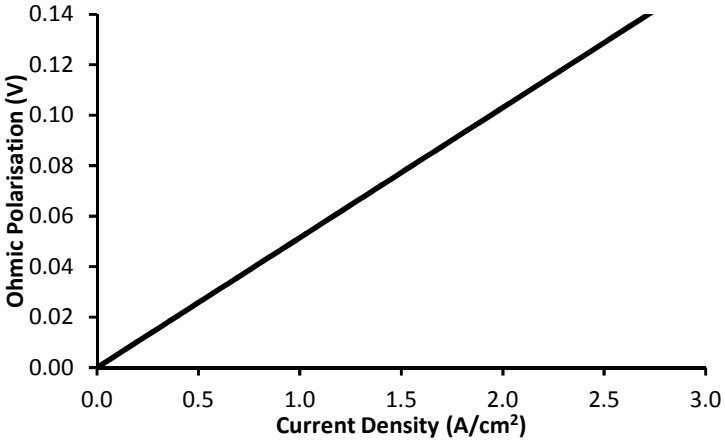

Figure 7: Ohmic polarisation

It can be seen from Equations 4 and 6 that the most significant contribution to cell potential loss is from the cathode side due to its high activation polarisation which results from the high activation energy needed to overcome the oxygen ion charge transfer reaction which is typically very slow. However the contribution of anode polarisation as seen in Figure 5 and ohmic loss in the electrolyte as seen in Figure 7 increases at increasing current density. The contribution of concentration polarisation in the anode is significant due to the comparatively thick diffusion layer which also serves as the support structure for the cell. The ohmic loss shown in Figure 7 is summed up as the cell potential losses due to the resistance of flow electrons and ions in the electrodes reaction layer, resistance of flow of electrons in the electrodes diffusion layers (both of which are usually small and insignificant) and the resistance of ion transport through the electrolyte layer (significant

6. CONCLUSION

The solution obtained from the numerical implementation of the two dimensional, along the channel, microscale, steady state, isothermal SOFC model is presented. The electrochemical model was first validated with measured experimental data and simulated data published in literature by measuring the cell performance. The developed model was then used to predict the performance of the anode supported SOFC operating at intermediate temperature. Simulation results show that the activation polarisation dominates the performance of the cell especially on the cathode side due to its significantly smaller exchange current density and the sluggishness of the oxygen reduction reaction. The ohmic polarisation is also important but less significant in this case because of the very thin electrolyte. The activation and ohmic polarisation are responsible for most of the cell voltage loss. The model presented in this paper illustrates the importance of polarisation modelling to identify the significant losses in the cell performance with a view to optimising and improving the SOFCs performance.

7. CONFLICT OF INTEREST

There is no conflict of interest associated with this work.

REFERENCES

Aguiar, P., Adjiman, C.S. and Brandon, N.P. (2004). Anode-supported intermediate temperature direct internal reforming solid oxide fuel cell. I: model-based steady-state performance. *Journal of Power Sources*, *138*(1), pp. 120-136.

Andersson, M., Yuan, J. and Sunden, B. (2012). SOFC modeling considering electrochemical reactions at the active three phase boundaries. *International Journal of Heat and Mass Transfer*, *55*(4), pp. 773-788.

Chinda, P., Chanchaona, S., Brault, P. and Wechsatol, W. (2010). Mathematical modeling of a solid oxide fuel cell with nearly spherical-shaped electrode particles. *Journal of Sustainable Energy & Environment*, *1*(4), pp. 185-196.

Costamagna, P., Costa, P. and Antonucci, V. (1998). Micro-modelling of solid oxide fuel cell electrodes. *Electrochimica Acta*, *43*(3), pp. 375-394.

Hussain, M.M., Li, X. and Dincer, I. (2006). Mathematical modeling of planar solid oxide fuel cells. *Journal of Power Sources*, *161*(2), pp. 1012-1022.

Jung, H.Y., Kim, W.S., Choi, S.H., Kim, H.C., Kim, J., Lee, H.W. and Lee, J. H. (2006). Effect of cathode current-collecting layer on unit-cell performance of anode-supported solid oxide fuel cells. *Journal of Power Sources*, *155*(2), pp. 145-151.

Larminie, J., Dicks, A. and McDonald, M.S. (2003). *Fuel cell systems explained* (Vol. 2). Chichester, UK: J. Wiley.

Ni, M., Leung, M.K.H. and Leung, D.Y.C. (2007). Micro-Scale Modeling of a Functionally Graded Ni-YSZ Anode. *Chemical Engineering & Technology*, *30*(5), pp. 587-592.

Ormerod, R.M. (2003). Solid oxide fuel cells. *Chemical Society Reviews*, *32*(1), pp. 17-28.

Singhal, S.C. and Kendall, K. (Eds.). (2003). *High-temperature solid oxide fuel cells: fundamentals, design and applications*. New York: Elsevier Advanced Technology. Xvi, 405, pp. 88-91.

Staniforth, J. and Ormerod, R.M. (2002). Implications for using biogas as a fuel source for solid oxide fuel cells: internal dry reforming in a small tubular solid oxide fuel cell. *Catalysis letters*, *81*(1), pp. 19-23.

Yakabe, H., Ogiwara, T., Hishinuma, M. and Yasuda, I. (2001). 3-D model calculation for planar SOFC. *Journal of Power Sources*, *102*(1), pp. 144-154.